



A LETTERS JOURNAL EXPLORING
THE FRONTIERS OF PHYSICS

OFFPRINT

Surface elastic properties in silicon nanoparticles

CLAUDIO MELIS, STEFANO GIORDANO and LUCIANO COLOMBO

EPL, **119** (2017) 66005

Please visit the website
www.epljournal.org

Note that the author(s) has the following rights:

- immediately after publication, to use all or part of the article without revision or modification, **including the EPLA-formatted version**, for personal compilations and use only;
- no sooner than 12 months from the date of first publication, to include the accepted manuscript (all or part), **but not the EPLA-formatted version**, on institute repositories or third-party websites provided a link to the online EPL abstract or EPL homepage is included.

For complete copyright details see: <https://authors.eplletters.net/documents/copyright.pdf>.

Surface elastic properties in silicon nanoparticles

CLAUDIO MELIS¹, STEFANO GIORDANO² and LUCIANO COLOMBO¹

¹ *Department of Physics, University of Cagliari, Cittadella Universitaria - I-09042 Monserrato (CA), Italy*

² *Institute of Electronics, Microelectronics and Nanotechnology - UMR 8520, LIA LICS, Univ. Lille, CNRS, Centrale Lille, ISEN, Univ. Valenciennes - F-59000 Lille, France*

received 23 June 2017; accepted in final form 15 November 2017

published online 6 December 2017

PACS 68.35.-p – Solid surfaces and solid-solid interfaces: structure and energetics

PACS 62.20.D- – Elasticity

PACS 68.35.Gy – Mechanical properties; surface strains

Abstract – The elastic behavior of the external surface of a solid body plays a key role in nanomechanical phenomena. While bulk elasticity enjoys the benefits of a robust theoretical understanding, many surface elasticity features remain unexplored: some of them are here addressed by blending together continuum elasticity and atomistic simulations. A suitable readdressing of the surface elasticity theory allows to write the balance equations in arbitrary curvilinear coordinates and to investigate the dependence of the surface elastic parameters on the mean and Gaussian curvatures of the surface. In particular, we predict the radial strain induced by surface effects in spherical and cylindrical silicon nanoparticles and provide evidence that the surface parameters are nearly independent of curvatures and, therefore, of the surface conformation.

Copyright © EPLA, 2017

The elastic behavior a solid body is ruled over by its bulk-like properties. This is reflected by the cardinal equation valid in its volume region Ω [1]

$$\frac{\partial T_{ik}}{\partial x_k} + b_i = \rho \frac{\partial^2 U_i}{\partial t^2}, \quad (1)$$

where ρ is the volume mass density, $T_{ik}(\vec{r}, t)$ is the three-dimensional Cauchy stress tensor, $U_i(\vec{r}, t)$ is the displacement vector, $b_i(\vec{r}, t)$ is the applied body force, $\vec{r} = (x_1, x_2, x_3)$ is the position vector within Ω and t is time (latin indexes indicate vector components). The corresponding continuum constitutive equation is written in the general form $\hat{T} = f(\hat{E})$ [2], provided that the strain tensor $E_{jh} = \frac{1}{2}(\frac{\partial U_j}{\partial x_h} + \frac{\partial U_h}{\partial x_j})$ is defined assuming the small deformation approximation. For a homogeneous and isotropic linear elastic body a universal constitutive equation is obtained

$$T_{ij} = 2\mu E_{ij} + \lambda \delta_{ij} E_{rr}, \quad (2)$$

where λ and μ are referred to as the bulk elastic constants [1,2]. Bulk linear elasticity is basically all contained in eqs. (1) and (2).

The surface Σ behaves differently from the volume Ω it delimits. This is inherently related to the very structure of a surface, where atoms are under-coordinated. They are, therefore, forced to relax in order to recover, at least

partially, the bulk-like value of their configurational energy. Unlike consequences of the relaxation processes occur perpendicular to the surface or parallel to it: in the first case, atoms mostly relax inwards towards the bulk, while atomic rearrangements on the surface are constrained by their mutual interactions. This results in the onset of a surface tension, at work even in the absence of any loading, which has no counterpart in bulk elasticity [3,4]. Because of this, surface elasticity is a much more challenging problem for theory than its bulk equivalent.

As a matter of fact, the actual features of a general surface constitutive equation are still a matter of investigation [5]. In particular, when a given material is considered, the dependence of the surface elastic parameters on the mean and Gaussian surface curvatures remains unexplored. Surface mechanics originates from the pioneer works by Laplace [6], Young [7], and Poisson [8], where the surface tension for fluids was introduced and the corresponding boundary-value problems were considered. Later, Gibbs generalized the notion of surface tension in the case of solids [9,10]. More recently, the seminal work by Gurtin and Murdoch [11,12] has paved the way to the modern description of the surface elasticity within the framework of rational mechanics. While several distinct approaches can be found in the literature [13–17], a unifying and comprehensive review can be found in ref. [18]. The requirement of a robust understanding of

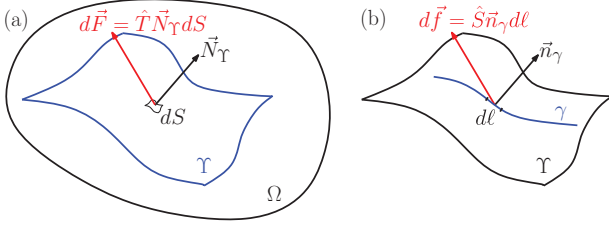


Fig. 1: (Colour online) Definition of (a) the three-dimensional stress tensor \hat{T} transmitting forces through a surface Υ (element dS) and (b) the two-dimensional stress tensor \hat{S} transmitting forces across a line γ (element $d\ell$). The forces are applied to the regions pointed by the vectors $-\vec{N}_\Upsilon$ or $-\vec{n}_\gamma$.

surface elasticity and stress fields has been recently called for by the need to understand and control a large variety of nano-scale physical phenomena, including: surface evolution [19], reconstruction and growth of surfaces [20], alloy segregation [21], phase transformation [22], stiffness of cantilever beams and films [23–25], contact mechanics with surface tension [26], capillarity effects in an elastic fluid [27–29], and mechanical behavior of nanocomposites [30–32], to name just a few.

This state of affairs motivates the present readdressing of the surface elasticity problem by treating Σ as a smooth Riemannian manifold and by adopting arbitrary curvilinear coordinates [33–35]. Upon derivation of the surface counterparts of eq. (1), we consider a linear and isotropic constitutive behavior (formulated in terms of two surface moduli λ_s and μ_s , and an intrinsic surface stress T_0) and, eventually, we work out a useful form of the balance equations for body and surface forces. The resulting continuum picture is then applied to predict the radial strain ϵ_R in spherical and cylindrical nanoparticles, differing as for the topological features of their surface. Atomistic simulations are next used to accomplish two tasks, namely: i) to calculate the actual value of λ_s , μ_s , and T_0 in a realistic case with planar surfaces; ii) to compute ϵ_R in variously sized and curved particles with no assumption on the underlying constitutive elastic behavior. Finally, a comparison is drawn between the continuum predictions for ϵ_R and atomistic results for silicon nanoparticles, enlightening the possible dependence of λ_s , μ_s , and T_0 on curvature.

Any curved surface Σ can be described in parametric form by $\vec{r} = \vec{r}(\alpha_1, \alpha_2)$ where α_1 and α_2 are real parameters. We define the metric tensor (first fundamental form) $g_{ij} = \frac{\partial \vec{r}}{\partial \alpha_i} \cdot \frac{\partial \vec{r}}{\partial \alpha_j}$, measuring the lengths over the surface via $d\ell^2 = g_{ij} d\alpha_j d\alpha_j$ (implicit sum over repeated indices) [33,34]. The inverse metric tensor g^{hk} is defined by $g^{ik} g_{kj} = \delta_j^i$. While the tangent base is composed of vectors $\vec{e}_i = \frac{\partial \vec{r}}{\partial \alpha_i}$, the cotangent one contains the vectors $\vec{e}^i = g^{ij} \vec{e}_j$. A vector \vec{v} defined over Σ can be therefore represented as $\vec{v} = v^i \vec{e}_i = v_i \vec{e}^i$, where v_i are the contravariant components and v^i are the covariant ones. Moreover, we can easily prove that $\|\vec{e}_i\| = \sqrt{g_{ii}}$ and $\|\vec{e}^j\| = \sqrt{g^{jj}}$ [34].

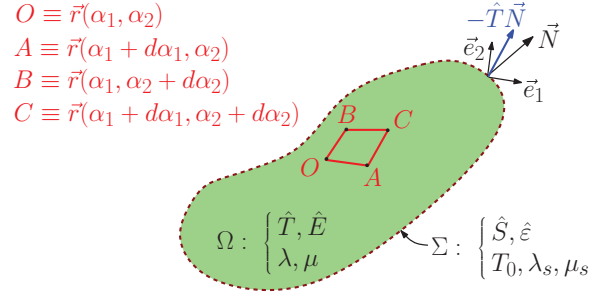


Fig. 2: (Colour online) A solid body of volume Ω is delimited by a surface Σ . For both entities the pertinent elastic fields and material parameters are indicated. The parallelogram $OACB$ on Σ is used to derive the balance equations. On each surface point the base $\{\vec{e}_1, \vec{e}_2, \vec{N}\}$ is defined and used, *e.g.*, to represent the $-\hat{T}\vec{N}$ stress vector locally applied to Σ .

We properly define the stress tensor for volumes and surfaces as follows (see fig. 1 for details). A solid material Ω is able to transmit a force $d\vec{F}$ through the area element dS of a given surface Υ by means of a (three-dimensional) stress tensor \hat{T} (measured in units $[\text{N}/\text{m}^2]$) defined as $d\vec{F} = \hat{T} \vec{N}_\Upsilon dS$ (with \vec{N}_Υ unit vector such as $\vec{N}_\Upsilon \perp \Sigma$) [1,2]. Moreover, a surface Υ in the solid material is able to transmit a force $d\vec{f}$ through the linear element $d\ell$ of a given line $\gamma \in \Upsilon$ by means of a (two-dimensional) stress tensor \hat{S} (measured in units $[\text{N}/\text{m}]$) defined as $d\vec{f} = \hat{S} \vec{n}_\gamma d\ell$ (with \vec{n}_γ unit vector such as $\vec{n} \perp \gamma$ and $\vec{n} \parallel \Upsilon$) [9,11].

Now, we take into account a solid body of volume Ω delimited by a surface Σ (see fig. 2). Then we consider on Σ the point $O \equiv \vec{r}(\alpha_1, \alpha_2)$ and the parallelogram composed of the point O and the neighbouring points $A \equiv \vec{r}(\alpha_1 + d\alpha_1, \alpha_2)$, $B \equiv \vec{r}(\alpha_1, \alpha_2 + d\alpha_2)$ and $C \equiv \vec{r}(\alpha_1 + d\alpha_1, \alpha_2 + d\alpha_2)$. We observe that $OA = \sqrt{g_{11}} d\alpha_1$ and $OB = \sqrt{g_{22}} d\alpha_2$. Also, we note that $\vec{e}^2 \perp \vec{e}_1$ and $\vec{e}^1 \perp \vec{e}_2$. We now determine the total force applied to the parallelogram $OACB$. It is composed of surface terms and volume terms.

We start by considering the surface contributions to the force, *i.e.*, the force applied from the region of Σ external to $OACB$ to the region $OACB$ itself. Of course, there are four surface terms corresponding to the infinitesimal segments OA , AC , CB and OB . For each term we use the expression $d\vec{f} = \hat{S} \vec{n}_\gamma d\ell$, previously introduced. We begin by calculating the force transmitted through the segment OA , which can be written as $d\vec{f}_{OA}^i = S^{ij} n_j d\ell$, where $d\ell = \sqrt{g_{11}} d\alpha_1$ and $\vec{n} = -\frac{1}{\sqrt{g^{22}}} \vec{e}^2$. It means that, on the cotangent base, we have $n_1 = 0$ and $n_2 = -\frac{1}{\sqrt{g^{22}}}$. Hence, we can write

$$d\vec{f}_{OA} = - \left(S^{12} \sqrt{\frac{g_{11}}{g^{22}}} \vec{e}_1 + S^{22} \sqrt{\frac{g_{11}}{g^{22}}} \vec{e}_2 \right) d\alpha_1. \quad (3)$$

Since $\sqrt{\frac{g_{11}}{g^{22}}} = \sqrt{\frac{g_{22}}{g^{11}}} = \sqrt{g_{11}g_{22} - g_{12}^2} = \sqrt{g}$, we have the

simplified expression

$$d\vec{f}_{OA} = -(S^{12}\vec{e}_1 + S^{22}\vec{e}_2) \sqrt{g} d\alpha_1. \quad (4)$$

To obtain $d\vec{f}_{CB}$ we can use the expression for $d\vec{f}_{OA}$, with opposite sign and calculated in $(\alpha_1, \alpha_2 + d\alpha_2)$. Its first-order development reads

$$d\vec{f}_{CB} = (S^{12}\vec{e}_1 + S^{22}\vec{e}_2) \sqrt{g} d\alpha_1 + \frac{\partial}{\partial \alpha_2} [(S^{12}\vec{e}_1 + S^{22}\vec{e}_2) \sqrt{g}] d\alpha_1 d\alpha_2. \quad (5)$$

Similar expressions can be found for $d\vec{f}_{OB}$ and $d\vec{f}_{AC}$, and the total surface force on the parallelogram $OACB$ is eventually given by

$$d\vec{f}_s = \frac{\partial}{\partial \alpha_k} (S^{ik} \vec{e}_i \sqrt{g}) d\alpha_1 d\alpha_2. \quad (6)$$

We now determine the volume force applied to the same parallelogram $OACB$. We consider the general expression $d\vec{F} = \hat{T}\vec{N}dS$, where $dS = \sqrt{g}d\alpha_1d\alpha_2$ for the infinitesimal parallelogram. The total volume force is generated by both the regions above (in the direction of \vec{N}) and below (in the direction of $-\vec{N}$) the surface Σ . We define $\Delta\hat{T} = \hat{T}^+ - \hat{T}^-$, where \hat{T}^\pm is the value of the volume stress tensor just above (below) the surface Σ . Hence, we can write

$$d\vec{f}_v = \Delta\hat{T}\vec{N}dS = [(\Delta T_n)\vec{N} + (\Delta T^1)\vec{e}_1 + (\Delta T^2)\vec{e}_2] \sqrt{g} d\alpha_1 d\alpha_2, \quad (7)$$

where ΔT^1 , ΔT^2 and ΔT_n are the components of the vector $\Delta\hat{T}\vec{N}$ on the base $\{\vec{e}_1, \vec{e}_2, \vec{N}\}$. If the surface Σ is free (no externally applied forces), we have that $\hat{T}^+ = 0$ and $\hat{T}^- = \hat{T}$ (internal stress). In this case, the components $(\Delta T^1, \Delta T^2, \Delta T_n)$ represent the vector $-\hat{T}\vec{N}$ on the base $\{\vec{e}_1, \vec{e}_2, \vec{N}\}$ of the surface Σ , as shown in fig. 2.

The Newton equation for the portion of surface within the parallelogram $OACB$ can be finally written as $d\vec{f}_s + d\vec{f}_v = \sigma \sqrt{g} d\alpha_1 d\alpha_2 \frac{\partial^2 \vec{U}}{\partial t^2}$, where σ is the surface mass density and \vec{U} represents the displacement vector. Its value $\vec{U} = \vec{U}(\vec{r}(\alpha_1, \alpha_2), t)$ over the surface Σ can be represented on the base $\{\vec{e}_1, \vec{e}_2, \vec{N}\}$ as $\vec{U} = u_n(\alpha_1, \alpha_2, t)\vec{N} + u^i(\alpha_1, \alpha_2, t)\vec{e}_i$. Therefore, the motion equation can be rewritten as

$$\frac{\partial S^{ik}}{\partial \alpha_k} \vec{e}_i + S^{ik} \left\{ \begin{matrix} s \\ ik \end{matrix} \right\} \vec{e}_s + S^{ik} f_{ik} \vec{N} + S^{ik} \left\{ \begin{matrix} j \\ kj \end{matrix} \right\} \vec{e}_j + (\Delta T_n)\vec{N} + (\Delta T^i)\vec{e}_i = \sigma \frac{\partial^2 u_n}{\partial t^2} \vec{N} + \sigma \frac{\partial^2 u^i}{\partial t^2} \vec{e}_i. \quad (8)$$

Here, we used the Gauss formula [33]

$$\frac{\partial \vec{e}_i}{\partial \alpha_k} = \frac{\partial^2 \vec{r}}{\partial \alpha_i \partial \alpha_k} = \left\{ \begin{matrix} s \\ ik \end{matrix} \right\} \vec{e}_s + f_{ik} \vec{N}, \quad (9)$$

and the property $\partial \sqrt{g} / \partial \alpha_k = \sqrt{g} \left\{ \begin{matrix} j \\ kj \end{matrix} \right\}$ [34], where the quantity $\left\{ \begin{matrix} s \\ ik \end{matrix} \right\}$ is the Christoffel symbol and the tensor

$f_{ik} = \frac{\partial^2 \vec{r}}{\partial \alpha_i \partial \alpha_k} \cdot \vec{N}$ is the shape tensor (second fundamental form) of the surface [33]. We can now separate the components in eq. (8), eventually obtaining the equations

$$S_{\parallel k}^{ik} + \Delta T^i = \sigma \frac{\partial^2 u^i}{\partial t^2}, \quad (10)$$

$$S^{ik} f_{ik} + \Delta T_n = \sigma \frac{\partial^2 u_n}{\partial t^2}, \quad (11)$$

where $S_{\parallel k}^{ik}$ is the covariant divergence of the Cauchy surface stress tensor S^{ij} . These equations represent the balance of forces on Σ , *i.e.*, the surface counterpart of eq. (1) holding within the volume Ω (see fig. 2). More specifically, eq. (10) describes the in-plane equilibrium, whereas eq. (11) describes the out-of-plane equilibrium.

The local stress on the surface must be related to the local surface deformation through a constitutive law. So, we need to define the strain tensor over the surface. When the surface is deformed by the displacement \vec{U} , the metric tensor becomes $g'_{kh} = \frac{\partial \vec{r}'}{\partial \alpha_k} \cdot \frac{\partial \vec{r}'}{\partial \alpha_h}$, where $\vec{r}' = \vec{r} + \vec{U}$. The calculation can be performed through the Gauss formula in eq. (9) and the Weingarten formula $\frac{\partial \vec{N}}{\partial \alpha_k} = -f_{ks} g^{sp} \vec{e}_p$ [33]. The result, to the first order in \vec{U} , is

$$g'_{kh} = g_{kh} - 2u_n f_{kh} + g_{ih} u_{\parallel k}^i + g_{ik} u_{\parallel h}^i, \quad (12)$$

where we used the covariant derivative of a vector $u_{\parallel k}^i$. The variation of the first form can be therefore written as $g'_{kh} = g_{kh} + 2\varepsilon_{kh}$, where we introduced the two-dimensional strain tensor

$$\varepsilon_{kh} = -u_n f_{kh} + \frac{1}{2} (g_{ih} u_{\parallel k}^i + g_{ik} u_{\parallel h}^i). \quad (13)$$

The geometrical meaning of ε_{kh} can be deduced by evaluating the relative variation of length in a given direction over the surface, under the applied displacement \vec{U} . Indeed, we easily get $\frac{d\ell' - d\ell}{d\ell} \cong \varepsilon_{kh} dt_k dt_h$, where $dt_k = d\alpha_k / \sqrt{g_{ij} d\alpha_i d\alpha_j}$ is the unit vector along which we measure the length variation. So, eq. (13) represents the standard definition of strain tensor, allowing the determination of length variation in a given spatial direction [36–38].

The relation between surface stress and surface strain (surface constitutive equation $\hat{S} = g(\hat{\varepsilon})$) can be written for linear and isotropic surfaces as

$$S^{ij} = -g^{ij} T_0 + \mu_s (g^{ir} g^{js} + g^{is} g^{jr}) \varepsilon_{rs} + \lambda_s g^{ij} g^{rs} \varepsilon_{rs}, \quad (14)$$

which is consistent with the tensor character of S^{ij} and ε_{rs} [36–38]. Here λ_s and μ_s are the surface elastic constants and T_0 is the intrinsic surface stress. These parameters are defined coherently with the literature [11,31].

We are interested in a more explicit form of eqs. (10) and (11) and, therefore, we combine eq. (13) with eq. (14). We directly obtain

$$S^{ij} = -g^{ij} T_0 + \mu_s (-2u_n g^{is} g^{jr} f_{rs} + g^{js} u_{\parallel s}^i + g^{ir} u_{\parallel r}^j) + \lambda_s (-u_n g^{ij} g^{rs} f_{rs} + g^{ij} u_{\parallel r}^r). \quad (15)$$

Now, we have to substitute this result in eqs. (10) and (11). To begin, we elaborate $S^{ij}f_{ij}$, as follows:

$$S^{ij}f_{ij} = -f_i^i T_0 + \mu_s(-2u_n f_r^i f_i^r + f_i^s u_{||s}^i + f_j^r u_{||r}^j) + \lambda_s(-u_n f_i^i f_j^j + f_i^i u_{||r}^r). \quad (16)$$

Then, we can calculate f_i^i and we get

$$f_i^i = g^{ij}f_{ij} = \text{Tr}(\hat{G}^{-1}\hat{F}) = \lambda_1 + \lambda_2 = 2H, \quad (17)$$

where \hat{G} and \hat{F} are the matrix representation of the first and second forms, respectively, λ_1 and λ_2 are the principal curvatures, and $H = (\lambda_1 + \lambda_2)/2$ is the mean curvature of Σ [33,35]. Moreover, we also calculate $f_r^i f_i^r$ by obtaining

$$\begin{aligned} f_r^i f_i^r &= g^{is} g^{jr} f_{rs} f_{ij} = \text{Tr}[(\hat{G}^{-1}\hat{F})^2] = \lambda_1^2 + \lambda_2^2 \\ &= (\lambda_1 + \lambda_2)^2 - 2\lambda_1\lambda_2 = (2H)^2 - 2K, \end{aligned} \quad (18)$$

where $K = \lambda_1\lambda_2$ is the Gaussian curvature of Σ [33,35]. Hence, the final form of $S^{ij}f_{ij}$ is the following:

$$S^{ij}f_{ij} = 2 \left\{ -HT_0 + \mu_s f_i^r u_{||r}^i + \lambda_s H u_{||r}^r + 2u_n [K\mu_s - H^2(\lambda_s + 2\mu_s)] \right\}. \quad (19)$$

The calculation of $S_{||k}^{ik}$ can be performed by observing that the covariant derivative follows the Leibniz product law and that the Ricci lemma can be applied for the covariant derivatives of the metric tensor ($g_{ij||k} = 0$ or $g_{||k}^{ij} = 0$) [34,35]. Straightforward calculations deliver the result

$$\begin{aligned} S_{||k}^{ik} &= -2u_n g^{ij} (\mu_s f_{||j}^{ij} + \lambda_s H g^{ij}) \\ &\quad - u_n (2\mu_s f_{||j}^{ij} + \lambda_s g^{ij} g^{rs} f_{rs||j}) \\ &\quad + \mu_s (g^{js} u_{||sj}^i + g^{ir} u_{||rj}^j) + \lambda_s g^{ij} u_{||rj}^r. \end{aligned} \quad (20)$$

Summing up, we can rewrite eq. (10) in the form

$$\begin{aligned} \sigma \frac{\partial^2 u^i}{\partial t^2} &= -2u_n g^{ij} (\mu_s f_{||j}^{ij} + \lambda_s H g^{ij}) \\ &\quad - u_n (2\mu_s f_{||j}^{ij} + \lambda_s g^{ij} g^{rs} f_{rs||j}) \\ &\quad + \mu_s (g^{js} u_{||sj}^i + g^{ir} u_{||rj}^j) + \lambda_s g^{ij} u_{||rj}^r + \Delta T^i, \end{aligned} \quad (21)$$

and eq. (11) as follows:

$$\begin{aligned} \sigma \frac{\partial^2 u_n}{\partial t^2} &= 2 \left\{ -HT_0 + \mu_s f_i^r u_{||r}^i + \lambda_s H u_{||r}^r \right. \\ &\quad \left. + 2u_n [K\mu_s - H^2(\lambda_s + 2\mu_s)] \right\} + \Delta T_n. \end{aligned} \quad (22)$$

Equations (21) and (22) are the surface counterparts of eqs. (1) and (2) and must be considered as the proper boundary conditions for any elastic problem defined in the region Ω . We remark that the static version of eq. (22) with $\lambda_s = 0$ and $\mu_s = 0$ represents the Young-Laplace equation $2HT_0 = \Delta T_n$, describing the capillary pressure difference sustained across the interface between

two static fluids [6,7]. It is important to remark that eqs. (21) and (22) are in perfect agreement with the Gurtin-Murdoch theory (under the assumption of small deformation elasticity) [11,12]. Nevertheless, we presented here an original and simpler derivation of these balance equations, and their explicit form in curvilinear coordinates, only based on the displacement components, is well suited for direct applications and numerical implementations. Moreover, they have the advantage to introduce the surface curvatures in a natural way, simplifying the analysis of specific cases, as discussed below.

The parameters λ_s , μ_s and T_0 are specific of each material forming the surface Σ with its given curvature. Some results for metals can be found in the literature [39,40]. Anyway, their systematic knowledge (even in the simpler model systems) is still missing and they are typically used as parametric values to tune by choice. To the aim of marking a conceptual step forward we addressed the surface elasticity problem by atomistic simulations. We selected amorphous silicon (a-Si) as show-case system, either because it is a technologically relevant material in many nanoscale problems and because the amorphous state of aggregation represents the atomistic counterpart of an isotropic elastic continuum. In other words, a-Si fully exploits the constitutive assumptions of eq. (14). More specifically, by a set of atomistic simulations we at first determine the bulk moduli λ and μ of a-Si; next we evaluate the corresponding elastic parameters λ_s , μ_s and T_0 for its planar surface; eventually we predict the strain distribution in specific a-Si nano-particles (spherical and cylindrical) with different curvatures. In order to elucidate the relationship between the surface elastic parameters and the surface curvatures, we will compare the continuum and atomistic results.

The bulk moduli λ and μ have been determined by means of model potential molecular dynamics (MPMD) using the LAMMPS [41] package and the environment-dependent interatomic potential (EDIP) [42]. The EDIP functional form consists of several coordination-dependent functions effectively matching Si-Si interactions to any possible bonding configuration. For this reason, it is particularly suitable for the description of non-crystalline systems such as a-Si. A sample A_0 was at first generated by constant-pressure and constant-temperature (NVT) quenching-from-the-melt protocol applied to a Si sample consisting in $75 \times 75 \times 75$ replicas of the diamond unit cell, corresponding to a total number of atoms as large as 3375000. The corresponding final mass density of simulated a-Si was 2.29 g/cm^3 , in perfect agreement with the experimental values [43]. Then, we applied to sample A_0 both uniaxial (along the [100], [010] and [001] directions) and hydrostatic deformations with an overall strain η varying in the range $\pm 2\%$ at intervals of 0.5% . At each deformation step the sample was fully relaxed by means of a NVT simulation over 150 ps (we used Nosé-Hoover thermostatting with a damping parameter of 100.0 fs and a time step as small as 1.0 fs) followed

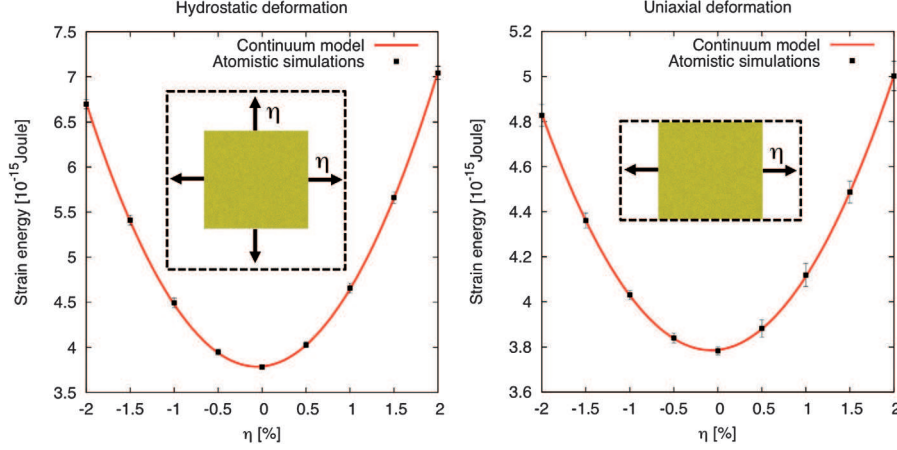


Fig. 3: (Colour online) Symbols: strain energy \mathcal{E}_{tot} obtained by MPMD as a function of the strain η for an a-Si slab subjected to the hydrostatic deformation (left panel) or the uniaxial deformation (right panel) shown in the insets. Full lines: strain energy provided by continuum theory and fitted to atomistic data through λ_s , μ_s and T_0 .

by a conjugate gradient optimization. In this case, periodic boundary conditions (PBC) along any direction were imposed. The optimization procedure of the structures was considered successful when one of the following criteria was met: i) the change in energy between two consecutive iterations was less than $e_{tol} = 1 \times 10^{-4}$ eV, or ii) the maximum force component (corresponding to each of the atoms) was smaller than $f_{tol} = 1 \times 10^{-6}$ eV/Å. We assessed the numerical convergence of the present minimization algorithm by verifying that the estimated values of the elastic properties were unchanged by considering a stricter minimization criterion ($e_{tol} = 1 \times 10^{-6}$ eV and $f_{tol} = 1 \times 10^{-8}$ eV/Å). The calculated values of λ and μ were 83 ± 2 and 26 ± 1 GPa, respectively, in very good agreement with previous results and experimental data [44].

We have thought up the evaluation of λ_s , μ_s and T_0 through a multi-step procedure, by targeting a planar slab of thickness h , area S_0 and volume $V_0 = hS_0$. Its bulk elasticity is described through the strain tensor $T_{ij} = \frac{\partial \mathcal{F}}{\partial E_{ij}}$, where \mathcal{F} is the strain energy density $\mathcal{F} = \mathcal{F}_0 + \frac{1}{2} \lambda E_{ii} E_{jj} + \mu E_{ij} E_{ij}$ (\mathcal{F}_0 is the energy density of the unstrained solid). The corresponding stress at the top and bottom surfaces is $S_{ij} = \frac{\partial \gamma}{\partial \varepsilon_{ij}}$, where γ is the surface strain energy density $\gamma = \gamma_0 - T_0 \varepsilon_{ii} + \frac{1}{2} \lambda_s \varepsilon_{ii} \varepsilon_{jj} + \mu_s \varepsilon_{ij} \varepsilon_{ij}$ (γ_0 is the corresponding density of the unstrained surface) [45]. By applying a planar strain $\hat{\varepsilon} = \text{diag}(\varepsilon_1, \varepsilon_2)$ to the slab, its bulk response takes the form of a deformation $\hat{E} = \text{diag}(\varepsilon_1, \varepsilon_2, \xi)$ and a corresponding stress $\hat{T} = \text{diag}(T_1, T_2, 0)$, where ξ is the vertical strain induced by the Poisson effect. The constitutive eq. (2) provides, after some algebra, an explicit result for the vertical strain, namely: $\xi = -\frac{\lambda}{2\mu + \lambda}(\varepsilon_1 + \varepsilon_2)$. Furthermore, the energy $\mathcal{E}_{bulk} = V_0 \mathcal{F}$ within the bulk can be fully calculated being function of λ and μ (previously evaluated), ε_1 and ε_2 (applied) and \mathcal{F}_0 (which can be easily found numerically). The total energy $\mathcal{E}_{tot} = 2\gamma S_0 + \mathcal{F} V_0$ of the slab is as well obtained through atomistic simulations, while the surface

energy is straightforwardly calculated as $\mathcal{E}_{surf} = \mathcal{E}_{tot} - \mathcal{E}_{bulk}$. By numerically evaluating such a surface energy for different applied strains, we can “measure” the elastic surface moduli: atomistic simulation is here conceived and used as a provider of raw data, in fact a sort of experiment providing rational phenomenology. A first option sets strain as $\hat{\varepsilon} = \text{diag}(\eta, \eta)$ (hydrostatic strain) and leads to the surface energy $\mathcal{E}_{surf} = 2S_0[\gamma_0 - 2T_0\eta + 2(\lambda_s + \mu_s)\eta^2]$; a second option sets $\hat{\varepsilon} = \text{diag}(\eta, 0)$ (uniaxial strain) and yields $\mathcal{E}_{surf} = 2S_0[\gamma_0 - T_0\eta + (\lambda_s/2 + \mu_s)\eta^2]$. The knowledge of the two curves (in a given range of η) allows to fit all the parameters describing the surface elasticity: indeed, the first curve is fully determined by the set $\{\gamma_0, -2T_0, 2(\lambda_s + \mu_s)\}$, while the second one engages the set $\{\gamma_0, -T_0, \lambda_s/2 + \mu_s\}$.

The above procedure has been put at work by loading sample A_0 with both hydrostatic and uniaxial deformations (see fig. 3) with a strain η varying in the range $\pm 2\%$ at intervals of 0.5%. In this case we applied PBC only along the directions parallel to the exposed surface, while free boundary conditions were set for the normal-to-surface direction. In order to increase statistics, we considered three different non-equivalent surfaces of the simulation supercell: all data have been accordingly averaged over three independent calculations. Eventually we obtained $T_0 = -1.28 \pm 0.05$ N/m, $\lambda_s = -30 \pm 5$ N/m and $\mu_s = -4 \pm 2$ N/m, respectively. As far as concerns T_0 , our results are in good agreement with previous *ab initio* calculations reporting $T_0 = -1.5 \pm 1.2$ N/m [46]. This validation stands for the robustness and reliability of the present procedure. On the other hand, to the best of our knowledge this is the first estimate ever of surface moduli λ_s and μ_s in a-Si.

The theoretical picture developed so far enables the determination of the strain distribution in spherical or cylindrical nano-particles with given radius R (for the cylinder we consider the configuration with fixed length). In both

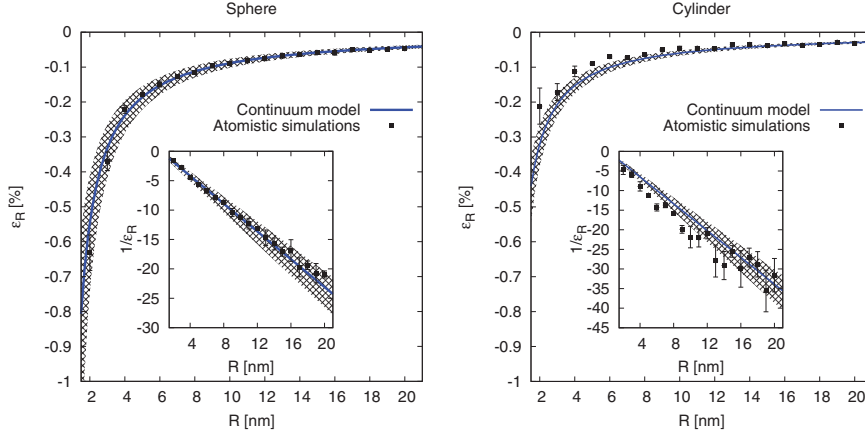


Fig. 4: (Colour online) Radial strain ϵ_R for spherical (left panel) and cylindrical (right panel) a-Si nano-particles of radius R computed atomistically by MPMD (symbols) and predicted by surface continuum elasticity (full lines). Filled areas represent the prediction range of the continuum model by taking into account the T_0 , λ_s and μ_s confidence interval ($\pm 3\sigma$).

geometries, continuum theory provides the radial displacement field as $\vec{U} = \epsilon_R r \vec{N}$, where $r^2 = x^2 + y^2 + z^2$ for the sphere and $r^2 = x^2 + y^2$ for the cylinder [47,48]. In both cases ϵ_R is the unknown radial strain. On both surfaces we have $u_n = \epsilon_R R$ and $u^i = 0$ ($i = 1, 2$). It is straightforward to prove that such a strain distribution exactly fulfills eq. (21) for both spherical and cylindrical particles. Therefore, the unknown radial strain ϵ_R can be determined through eq. (22), which in a static regime assumes the simplified form

$$0 = -2HT_0 + 4u_n [K\mu_s - H^2(\lambda_s + 2\mu_s)] + \Delta T_n, \quad (23)$$

where it has been set $u^i = 0$ ($i = 1, 2$). For the sphere we have $u_n = \epsilon_R R$, $\Delta T_n = -\hat{T} \vec{N} \cdot \vec{N} = -\epsilon_R (3\lambda + 2\mu)$, and the curvatures $H = -1/R$ and $K = 1/R^2$. Hence, eq. (23) can be solved eventually obtaining the radial strain as

$$\epsilon_R = \frac{2T_0}{4(\lambda_s + \mu_s) + (3\lambda + 2\mu)R}. \quad (24)$$

Similarly, for the cylinder we have $u_n = \epsilon_R R$, $\Delta T_n = -\hat{T} \vec{N} \cdot \vec{N} = -2\epsilon_R(\lambda + \mu)$, $H = -\frac{1}{2R}$ and $K = 0$ driving to

$$\epsilon_R = \frac{T_0}{(\lambda_s + 2\mu_s) + 2(\lambda + \mu)R}. \quad (25)$$

Results in eqs. (24) and (25) agree with the previous literature [49,50] and can be directly compared with atomistic simulations. In detail, both a spherical and a cylindrical a-Si sample with increasing size were carved out from the sample A_0 . In both cases we considered 19 samples with $2 \text{ nm} \leq R \leq 20 \text{ nm}$ and, for cylinders, we set length to $L_z = 40.9 \text{ nm}$. We imposed free boundary conditions along all directions, but along the cylinder axis where PBC have been imposed. All the samples have been fully relaxed as above. The radial strain ϵ_R was estimated by $\epsilon_R = \frac{1}{N} \sum_{i=1}^N \epsilon_R^i = \frac{1}{N} \sum_{i=1}^N \frac{R^i - R_0^i}{R_0^i}$, where N is the number of atoms in the sample, while R_0^i and R^i is the distance

of the i -th atom from the sphere center or cylinder axis, respectively before and after relaxation. For each system of given dimension we performed 5 independent calculations: data reported in fig. 4 represent the configurational averages and are compared with continuum results stated in eqs. (24) (sphere) and (25) (cylinder). Continuum results are based on the parameters λ_s , μ_s and T_0 previously obtained for the planar slab. The red filled areas represent the prediction range of the continuum model: this reflects the dependence of the elastic parameters on local details of the underlying amorphous structure.

In conclusion, we have worked out a universal local representation for the equations describing the elasticity of any arbitrarily curved solid surface and defined an atomistic protocol for determining the relevant elastic parameters. Full agreement between atomistics and continuum is found for differently shaped a-Si nanoparticles, providing evidence that the surface elastic parameters are nearly independent of the surface curvatures. This is a significant result since the a-Si surface elastic parameters can be evaluated for an arbitrarily curved surface and remain valid for any other surface with different conformation. This strongly facilitates the analysis of mechanical problems with surface elasticity.

REFERENCES

- [1] ATKIN R. J. and FOX N., *An Introduction to the Theory of Elasticity* (Dover Publication Inc., New York) 1980.
- [2] LANDAU L. D. and LIFSHITZ E. M., *Theory of Elasticity* (Butterworth Heinemann, Oxford) 1986.
- [3] CAMMARATA R. C., *Prog. Surf. Sci.*, **46** (1994) 1.
- [4] MÜLLER P. and SAÚL A., *Surf. Sci. Rep.*, **54** (2004) 157.
- [5] DINGREVILLE R. and QU J., *Acta Mater.*, **55** (2007) 141.
- [6] LAPLACE P. S., in *Traité de Mécanique Celeste*, Vol. 4 Supplement 1, Livre X (Gauthier-Villars, Paris) 1805, pp. 771–777.

- [7] YOUNG T., *Philos. Trans. R. Soc. London*, **95** (1805) 65.
- [8] POISSON S. D., *Nouvelle théorie de l'action capillaire* (Bachelier Père et Fils, Paris) 1831.
- [9] GIBBS J. W., in *The Collected Works of J. W. Gibbs*, Vol. **1** (Longmans, New York) 1928, p. 315.
- [10] OLIVES J., *J. Phys.: Condens. Matter*, **22** (2010) 085005.
- [11] GURTIN M. E. and MURDOCH A. I., *Arch. Ration. Mech. Anal.*, **57** (1975) 291; **59** (1975) 389.
- [12] GURTIN M. E. and MURDOCH A. I., *Int. J. Solids Struct.*, **14** (1978) 431.
- [13] SHARMA P., GANTI S. and BHATE N., *Appl. Phys. Lett.*, **82** (2003) 535.
- [14] CHEN T., CHIU M.-S. and WENG C.-N., *J. Appl. Phys.*, **100** (2006) 074308.
- [15] CHEN T., DVORAK G. J. and YU C. C., *Acta Mech.*, **188** (2007) 39.
- [16] STEIGMANN D. J. and OGDEN R. W., *Proc. R. Soc. A*, **455** (1999) 437.
- [17] MÜLLER P., SAÛL A. and LEROY F., *Adv. Nat. Sci.: Nanosci. Nanotechnol.*, **5** (2014) 013002.
- [18] JAVILI A., MCBRIDE A. and STEINMANN P., *Appl. Mech. Rev.*, **65** (2013) 010802.
- [19] FREUND L. B. and SURESH S., *Thin Film Materials* (Cambridge University Press, Cambridge) 2003.
- [20] IBACH H., *Surf. Sci. Rep.*, **29** (1997) 195; **35** (1999) 71.
- [21] SCHMID M., HOFER W., VARGA P., STOLTZE P., JACOBSEN K. W. and NORSKOV J. K., *Phys. Rev. B*, **51** (1995) 10937.
- [22] DIAO J., GALL K. and DUNN M. L., *Nat. Mater.*, **2** (2003) 656.
- [23] MILLER R. E. and SHENOY V. B., *Nanotechnology*, **11** (2000) 139.
- [24] DINGREVILLE R., QU J. and CHERKAoui M., *J. Mech. Phys. Sol.*, **53** (2005) 1827.
- [25] LACHUT M. J. and SADER J. E., *Phys. Rev. B*, **85** (2012) 085440.
- [26] STYLE R. W., HYLAND C., BOLTYANSKIY R., WETTLAUFRER J. S. and DUFRESNE E. R., *Nat. Commun.*, **4** (2013) 2728.
- [27] MINDLIN R. D., *Int. J. Sol. Struct.*, **1** (1965) 417.
- [28] FOREST S., CORDERO N. M. and BUSSO E. P., *Comput. Mater. Sci.*, **50** (2011) 1299.
- [29] NOZIÈRES P., in *Solids far from Equilibrium*, edited by GODRÈCME C. (Cambridge University Press, Cambridge) 1992, Chapt. 1.
- [30] DUAN H. L., WANG J., HUANG Z. P. and KARIHALOO B. L., *J. Mech. Phys. Solids*, **53** (2005) 1574.
- [31] DUAN H. L., WANG J. and KARIHALOO B. L., *Adv. Appl. Mech.*, **42** (2009) 1.
- [32] KOUTSAWA Y., TIEM S., YUC W., ADDIEGO F. and GIUNTA G., *Comp. Struct.*, **159** (2017) 278.
- [33] STRUIK D. J., *Lectures on Classical Differential Geometry* (Dover Publications, New York) 1988.
- [34] LEVI-CIVITA T., *The Absolute Differential Calculus* (Blackie & Son Limited, London) 1946.
- [35] SYNGE J. L. and SCHILD A., *Tensor Calculus* (Dover Publication Inc., New York) 1978.
- [36] MARSDEN J. E. and HUGHES T. J. R., *Mathematical Foundations of Elasticity* (Dover Publication Inc., New York) 1994.
- [37] GREEN A. E. and ZERNA W., *Theoretical Elasticity* (Oxford Press, Oxford) 1954.
- [38] CIARLET P. G., *An Introduction to Differential Geometry with Application to Elasticity* (Springer, Dordrecht) 2005.
- [39] WOLFER W. G., *Acta Mater.*, **59** (2011) 7736.
- [40] SHENOY V. B., *Phys. Rev. B*, **71** (2005) 094104.
- [41] PLIMPTON S., *J. Comp. Phys.*, **117** (1995) 1. See also the following site: <http://lammps.sandia.gov>.
- [42] JUSTO J. F., BAZANT M. Z., KAXIRAS E., BULATOV V. V. and YIP S., *Phys. Rev. B*, **58** (1998) 2539.
- [43] REMES Z., VANECEK M., TORRES P., KROLL U., MAHAN A. H. and CRANDALL R. S., *J. Non-Cryst. Solids*, **227** (1998) 876.
- [44] ALLRED C. L., YUAN X., BAZANT M. Z. and HOBBS L. W., *Phys. Rev. B*, **70** (2004) 134113.
- [45] MATTONI A., COLOMBO L. and CLERI F., *Phys. Rev. Lett.*, **95** (2005) 115501.
- [46] HARA S., IZUMI S., KUMAGAI T. and SAKAI S., *Surf. Sci.*, **585** (2005) 17.
- [47] LOVE A. E. H., *A Treatise on the Mathematical Theory of Elasticity* (Dover, New York) 2002.
- [48] SNEDDON I. N. and BERRY D. S., *The Classical Theory of Elasticity*, in *Elasticity and Plasticity*, edited by FLÜGGE S., Vol. **VI** (Springer-Verlag, Berlin) 1958, pp. 1–126.
- [49] MURDOCH A. I., *Q. J. Mech. Appl. Math.*, **29** (1976) 245.
- [50] MURDOCH A. I., *Int. J. Eng. Sci.*, **16** (1978) 131.